General Disclaimer

One or more of the Following Statements may affect this Document

- This document has been reproduced from the best copy furnished by the organizational source. It is being released in the interest of making available as much information as possible.

- This document may contain data, which exceeds the sheet parameters. It was furnished in this condition by the organizational source and is the best copy available.

- This document may contain tone-on-tone or color graphs, charts and/or pictures, which have been reproduced in black and white.

- This document is paginated as submitted by the original source.

- Portions of this document are not fully legible due to the historical nature of some of the material. However, it is the best reproduction available from the original submission.

MASSACHUSETTS INSTITUTE OF TECHNOLOGY
RESEARCH LABORATORY OF ELECTRONICS
Cambridge, Massachusetts 02139

Reprinted from
Quarterly Progress Report No. 101, April 15, 1971

The Research Laboratory of Electronics is an interdepartmental laboratory in which faculty members and graduate students from numerous academic departments conduct research.

The research reported in this document was made possible by support extended the Massachusetts Institute of Technology, Research Laboratory of Electronics, by the following agencies.

Joint Services Electronics Programs (U.S. Army, U.S. Navy, and U.S. Air Force)

Contract DA 28-043-AMC-02536(E)

U.S. Navy – Office of Naval Research

Contract N00014-67-A-0204-0033

U.S. Air Force – Electronics Systems Division

Contract F19628-69-C-0044
Contract F19628-70-C-0064

National Aeronautics and Space Administration

Grant NGL 22-009-337
Grant NGR 22-009-091

National Institutes of Health

Grant 5 PO1 GM14940-05
Grant 5 RO1 NS04332-08

National Institute of Mental Health

Grant 5 PO1 MH13390-05

National Science Foundation

Grant GK-18185

U.S. Atomic Energy Commission

Contract AT (30-1)-3980

Bell Telephone Laboratories Inc. (Grant)

M.I.T. Sloan Fund For Basic Research (Grant 241)

California Institute of Technology Contract No. 952568

Support of projects is acknowledged in footnotes to the appropriate sections.

III. PHYSICAL ELECTRONICS AND SURFACE PHYSICS*

Academic and Research Staff

Prof. R. E. Stickney
Dr. A. E. Dabiri

Graduate Students

P. C. Abbott
V. S. Aramati
T. L. Bradley
T. E. Kenney
C. N. Lu
D. V. Tendulkar

A. ANALYSIS OF THE "PUMPING" OF OXYGEN BY A TUNGSTEN FILAMENT IN A HOT-CATHODE IONIZATION GAUGE

1. Introduction

Accurate measurements of oxygen pressures below $\sim 1 \times 10^{-4}$ Torr are necessary in a variety of experimental investigations, such as studies of the pressure and composition of the upper atmosphere, the solubility, permeation, and degassing of oxygen in solids, the kinetics of oxidation, and the influence of adsorbed oxygen on the properties of solid surfaces. Most of the ionization gauges and mass spectrometers that are suitable for measuring pressure below $\sim 1 \times 10^{-4}$ Torr employ a hot cathode as the electron source.[1,2] Unfortunately, measurements of O_2 pressures with hot cathode gauges have proved to be unrealiable because of several problems.[1] One of the problems is that the pressure in the gauge may be substantially lower than in the test region because of the "pumping" of oxygen by the chemical reaction of O_2 with the hot cathode. The objective of the present paper is to develop an approximate analysis of this "pumping" effect.

We shall briefly review Singleton's work[3] because our analysis requires a detailed understanding of his experimental conditions, techniques, and measurements. The principal features of Singleton's apparatus are illustrated schematically in Fig. III-1. A tungsten filament having a total surface area of 4 cm^2 is heated resistively to temperature T. The total pressure, p, is measured with a modulated ion gauge, and the partial pressures, p_i, are measured with a cycloidal mass spectrometer (partial pressure analyzer). The partial pressure of O_2, p_{O_2}, is varied by adjusting a variable leak valve connected to a flask of high-purity O_2. For steady-state conditions with the filament unheated (i.e., $T \approx 300°K$), the rate of flow into the chamber, Q_{in}, is balanced by an equal flow out of the chamber, Q_{out}, which may be expressed as

*This work was supported principally by the National Aeronautics and Space Administration (Grant NGR 22-009-091), and in part by the Joint Services Electronics Programs (U.S. Army, U.S. Navy, and U.S. Air Force) under Contract DA 28-043-AMC-02536(E).

$$Q_{in} = Q_{out} = S_{O_2} p_{O_2}, \tag{1}$$

where S_{O_2} is the pumping speed of the apparatus for O_2 (0.43 l/sec).[4] Singleton found that p_{O_2} changed to a lower value, p'_{O_2}, when the filament temperature was increased while holding Q_{in} constant. This effect was first reported by Langmuir who offered

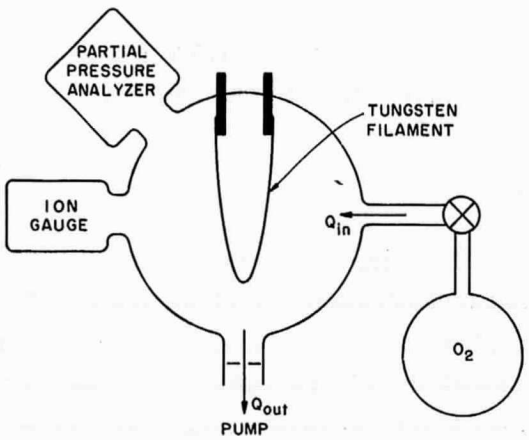

Fig. III-1. Singleton's experimental apparatus.

essentially the following explanation: A portion of the O_2 molecules are permanently removed ("pumped") from the gas phase as a result of chemical reaction of O_2 with the hot filament to form tungsten oxide molecules that evaporate from the filament and condense upon the chamber wall. Q_f, the rate at which O_2 is "pumped" by reaction with the hot filament, is usually expressed as

$$Q_f(\text{Torr-l/sec}) = \epsilon A Z_{O_2} = 11.1 \epsilon A p'_{O_2}, \tag{2}$$

where ϵ is defined as the fraction of the O_2 molecules impinging upon the filament that are "pumped" (i.e., the fraction that react to form volatile species that condense on the chamber wall), A is the total surface area of the filament, and $Z_{O_2} = 11.1\, p'_{O_2}$ (Torr-l/cm^2-sec) is the rate of impingement of O_2 per unit surface area, under the assumption that the gas temperature is equal to that of the chamber walls (~300°K). Therefore, for steady-state conditions with the filament at elevated temperature, Q_{in} is balanced by the sum of the pumping rates of the vacuum system and of the filament:

$$Q_{in} = S_{O_2} p'_{O_2} + 11.1 \epsilon A p'_{O_2} \tag{3}$$

Since Q_{in} is constant, Eq. 3 may be equated to Eq. 1 to eliminate Q_{in}, and the resulting expression may be solved for ϵ to yield

$$\epsilon = \frac{1}{11.1\,A}\left[S_{O_2}\left(p_{O_2}/p'_{O_2} - 1\right)\right] \tag{4a}$$

$$= 0.0097\left(p_{O_2}/p'_{O_2} - 1\right), \tag{4b}$$

where p_{O_2}/p'_{O_2} is the ratio of the steady-state O_2 partial pressures measured with the filament first at 300°K and then at an elevated temperature, T. Singleton derived the results shown in Fig. III-2 from experimental measurements of p_{O_2} and p'_{O_2} for a range of filament temperatures and O_2 pressures. Notice that ϵ depends on both T and p_{O_2}.

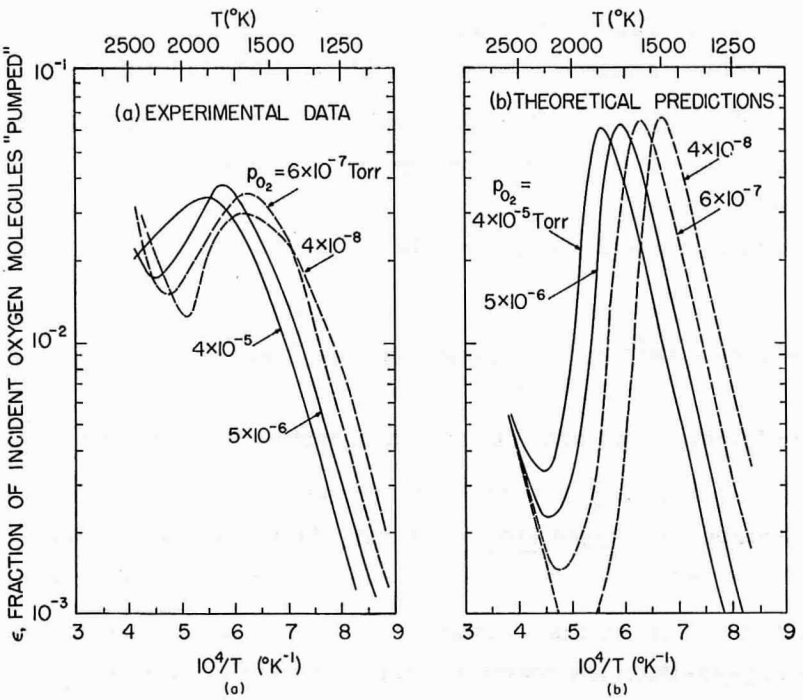

Fig. III-2. (a) Singleton's experimental data on the "pumping" of oxygen by a hot tungsten filament.
(b) Theoretical prediction of the "pumping" of oxygen by a hot tungsten filament.

2. Analysis

The first assumption of the quasi-equilibrium treatment[5, 6] is simply that a fraction (ζ'_{O_2}) of the impinging O_2 molecules is equilibrated to the tungsten surface, whereas

the remainder is scattered without chemical change; that is, they rebound as O_2 molecules. Based on a semi-empirical procedure, Batty and Stickney[6] have suggested the following approximate relation for ζ'_{O_2} in the case of tungsten at temperature T and O_2 at 300°K and pressure p'_{O_2}:

$$\zeta'_{O_2} = 80\,(p'_{O_2})^{-0.3} \exp(-18,400/T). \tag{5}$$

[Note: Since values of ζ'_{O_2} greater than unity are absurd, we shall assume $\zeta'_{O_2} = 1$ when Eq. 5 yields $\zeta'_{O_2} > 1$.] A possible physical interpretation of the increase of ζ'_{O_2} with increasing T and decreasing p'_{O_2} is the fact that these conditions cause the steady-state concentration of adsorbed oxygen atoms to decrease, thereby decreasing the probability that an incident O_2 molecule will fail to be equilibrated because of colliding with an adsorbed oxygen atom rather than with the bare tungsten surface. (See Batty and Stickney[5,6] for a more detailed discussion of ζ'_{O_2}.) Based on this expression for ζ'_{O_2}, Batty and Stickney[6] have shown that the results of the quasi-equilibrium analysis agree quite well with existing experimental data on the rate of removal of tungsten from hot filaments exposed to O_2.

The rate at which O_2 molecules equilibrate to the surface per unit area may be expressed as

$$\zeta'_{O_2} Z'_{O_2} = 3.59 \times 10^{20}\, \zeta'_{O_2} p'_{O_2} \text{ molecules cm}^{-2} \text{ sec}^{-1}, \tag{6}$$

where Z'_{O_2} is the impingement rate expressed in terms of molecules cm^{-2} sec^{-1} when p'_{O_2} is expressed in Torr and the gas is at the temperature of the chamber wall (300°K).[7] Therefore, the number of oxygen <u>atoms</u> entering the equilibrated adsorbate phase on the tungsten surface per cm^2 per sec is $2\zeta'_{O_2} Z'_{O_2}$. If steady-state conditions exist, then an equal number of oxygen atoms must leave the adsorbate per cm^2 per sec as volatile products of the oxygen-tungsten reactions (i.e., as O, O_2, WO, WO_2, ...). This conservation requirement may be stated as

$$2\zeta'_{O_2} Z'_{O_2} = \sum_{x,y} y\, R_{W_xO_y} \tag{7a}$$

$$= R_O + 2R_{O_2} + R_{WO} + 2R_{WO_2} + 3R_{WO_3}$$

$$+ 6R_{W_2O_6} + 8R_{W_3O_8} + 9R_{W_3O_9} + 12R_{W_4O_{12}}, \tag{7b}$$

where $R_{W_xO_y}$ represents the rate of evaporation of species W_xO_y. In Eq. 7b we have

included all of the species that are expected to be significant at high temperatures and low pressures. [It should be emphasized that since R_{O_2} represents the rate of evaporation of O_2 molecules from the equilibrated adsorbate phase, it does not include the rate at which the nonequilibrated O_2 molecules rebound from the surface per unit area, that is, $(1-\zeta'_{O_2})Z'_{O_2}$.]

The second assumption of the quasi-equilibrium treatment is that the chemical composition of the products evaporating from the surface is identical to that of an equilibrium mixture at the temperature of the solid. This means that the evaporation rates are related through the equilibrium constants, $K_p(T)$. Specifically, if the gas-solid reaction is described by a set of stoichiometric equations of the following generalized form

$$xW(s) + \frac{y}{2}\, O_2(g) \rightleftharpoons W_xO_y(g), \tag{8}$$

then the relation between the evaporation rates and the equilibrium constant is[8]

$$K_{W_xO_y}(T) = (2\pi kT)^{1/2(1-1/2y)} \left[\frac{m_{W_xO_y}}{m_{O_2}^{y/2}}\right]^{1/2} \frac{R_{W_xO_y}}{R_{O_2}^{y/2}}, \tag{9}$$

where m_i is the molecular mass of species i.

Since the values of $K_{W_xO_y}(T)$ may be taken directly from the JANAF Tables,[9] Eqs. 5 through 9 provide sufficient information to enable us to compute the evaporation rates for specified values of T and p'_{O_2}. We may then use these rates to predict the O_2 pumping speed of a hot tungsten filament as a function of T and p'_{O_2}. For example, if we assume that all of the tungsten oxides condense permanently upon the chamber wall but the O atoms recombine at the wall to form O_2 molecules that return to the gas phase, then ϵ may be predicted from the relation

$$\epsilon = \frac{\frac{1}{2}R_{WO} + R_{WO_2} + \frac{3}{2}R_{WO_3} + 3R_{W_2O_6} + 4R_{W_3O_8} + \frac{9}{2}R_{W_3O_9} + 6R_{W_4O_{12}}}{Z'_{O_2}}. \tag{10}$$

The results shown in Fig. III-2 were computed by this method. To simulate Singleton's experimental conditions, our calculations of Z'_{O_2} in Eqs. 6, 7, and 10 are based on the measured values of p'_{O_2}, rather than on the values of the initial pressure, p_{O_2}, given

in Fig. III-2. [Although Singleton did not directly report the measured values of p'_{O_2}, they are easily recovered from his data on ϵ (Fig. III-2a) by applying Eq. 4b.]

3. Discussion of Results

The most significant feature of Fig. III-2 is the similarity of the general shape of the predicted curves to that of the curves based on Singleton's experimental data. Both sets of curves are S-shaped with peaks occurring in the same temperature range (~1500-1800°K) and with magnitudes that differ by no more than approximately a factor of two at the peaks as well as at lower temperatures. This degree of agreement is as good as we should hope for considering the limited accuracy of the values of ζ'_{O_2} and $K_p(T)$ employed in the analysis. On the other hand, notice that at higher temperatures the discrepancies between the predicted curves and the corresponding experimental data are slightly greater than a factor of ten in some cases. Since we believe that discrepancies of this magnitude cannot be ascribed entirely to errors in ζ'_{O_2} or $K_p(T)$, several possible explanations will be considered.

According to Singleton,[3] the experimental results for $T > 1800°K$ are less reliable than those at lower temperatures because of the difficulty of obtaining reproducible data. A major problem was that steady-state conditions were not attained even after 10-20 h in some tests at high temperature and low pressure. Based on auxiliary experiments and approximate calculations, Singleton concluded that a fraction of the O atoms desorbed from the filament is "pumped" by adsorption on the chamber wall, and this fraction decreases with time because the wall becomes saturated. Since the theoretical predictions shown in Fig. III-2b are based on the assumption that none of the O atoms impinging upon the chamber wall are "pumped," this provides a consistent explanation for the fact that the predicted values of ϵ are smaller than the experimental results for temperatures above ~1800°K.

To modify our analysis to allow a fraction α of the O atoms to be "pumped," we need only to add the term $1/2\alpha\ R_O$ to the numerator of Eq. 10. As illustrated in Fig. III-3, the predicted values of ϵ are extremely sensitive to small changes in the value assumed for α. The curves for different values of α are essentially identical up to $T \approx 1800°K$ because R_O is negligible at lower temperatures. A detailed comparison of the predicted and experimental results for $T > 1800°K$ is not warranted, since we suspect that α is a complicated function of many variables (e.g., the temperatures of the filament and the walls, the O_2 pressure, the partial pressures of the residual gases, and the chemical composition of the chamber walls).

We should mention two other problems that may contribute to the discrepancy between the predicted and experimental results above ~1800°K. First, Singleton suggests that the reaction of O atoms with carbon or carbon containing components on the chamber

walls may be responsible for his experimental observation that the relative amount of CO in the chamber increases with increasing filament temperature and decreasing O_2 pressure. Since a reaction of this nature would result in a decrease in the O_2 pressure, it would cause the experimentally determined values of ϵ to be larger than the theoretical predictions. We are unable to estimate the magnitude of this effect because the necessary data are not available. A second problem is the pumping speed associated with adsorption ("gettering") of O_2 and O by the tungsten layer that forms continuously on the chamber wall as a result of sublimation from the hot filament. To obtain an estimate of the effect of this pumping process on the magnitude of ϵ, we shall assume

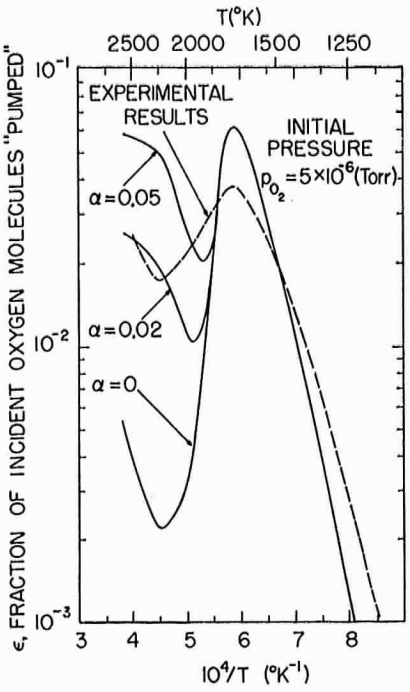

Fig. III-3.

Theoretical prediction of the "pumping" of oxygen by a hot tungsten filament for three values of α, the fraction of oxygen atoms that are "pumped" by adsorption on the chamber walls.

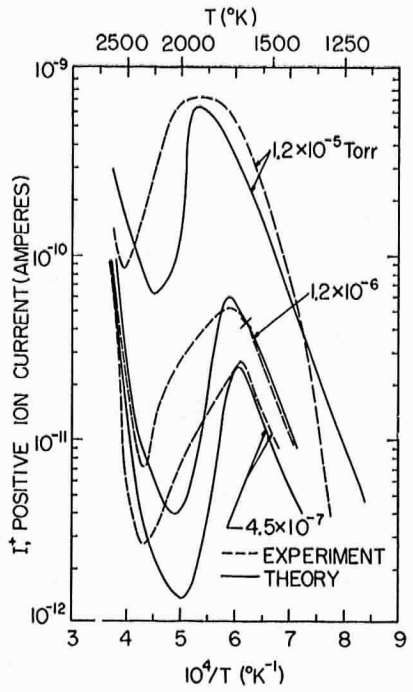

Fig. III-4.

Comparison of the predictions of the quasi-equilibrium model (solid curves) with the experimental data of Winters et al. for positive ion emission from a heated tungsten filament.

for simplicity that each tungsten atom getters one O_2 molecule. Based on this assumption, the increase in ϵ resulting from gettering is

$$\Delta\epsilon = R_W/Z'_{O_2} \approx 1.3\times10^{10}\, T^{-1/2} \left(p'_{O_2}\right)^{-1} 10^{-4.07\times10^4/T}, \qquad (11)$$

where R_W, the sublimation rate of tungsten, has been represented by an approximate empirical equation. Since $\Delta\epsilon$ will be greatest at the highest temperature and lowest pressure, we shall evaluate Eq. 11 at 2500°K and 4×10^{-8} Torr. The result is $\Delta\epsilon \approx 0.4$, which means that the value of $\epsilon \times 100$ corresponding to 2500°K and 4×10^{-8} Torr in Fig. III-2b would be increased from ~0.4 to ~40. This illustration leads to the conclusion that gettering may be the dominant pumping process at the highest temperatures and lowest pressures.

It seems worthwhile to point out that the quasi-equilibrium analysis also provides an approximate explanation of another process that occurs when a hot tungsten filament is exposed to O_2. This process is the evaporation of impurities from the filament especially those impurities that evaporate as ions (e.g., K^+, Na^+). Winters et al.[11] obtained the data shown in Fig. III-4, and they suggest that the observed dependence of ion emission on p_{O_2} results from the fact that the removal of tungsten by the O_2-W reaction increases with p_{O_2}, thereby increasing the rate of uncovering pockets of impurities that are distributed throughout the filament. If their suggestion is valid, then the ion emission current, I^+, should be proportional to Σ_W, the rate of removal of tungsten atoms from the filament surface by the combined processes of oxidation and sublimation, where

$$\Sigma_W \equiv \sum_{x,y} \times R_{W_xO_y} = R_W + R_{WO_2} + R_{WO_3} + 2R_{W_2O_6} + \ldots . \tag{12}$$

We have computed Σ_W on the basis of the quasi-equilibrium analysis described above, and the results are included in Fig. III-4. Since the constant of proportionality between I^+ and Σ_W was not known, we estimated it empirically by forcing the curves for I^+ and Σ_W to agree at a single point (denoted X in Fig. III-4). In this particular case, the constant is $I^+/\Sigma_W \approx 3 \times 10^{-24}$ A cm^2 sec, which means that the ratio of ions emitted to W atoms removed is $\sim 5 \times 10^{-5}$ if we assume that the surface area of the filament was 0.4 cm^2. (Note: the value of the constant vary substantially for filaments having different impurity levels and/or processing.) The agreement of the experimental and theoretical curves in Fig. III-4 is reasonably satisfactory in view of the simplicity of the model.

A. E. Dabiri, R. E. Stickney

References

1. P. A. Redhead, J. P. Hobson, and E. V. Kornelsen, The Physical Basis of Ultra-high Vacuum (Chapman and Hall, London, 1968), Chaps. 7, 8 and 9.
2. S. Dushman and J. M. Lafferty, Scientific Foundations of Vacuum Technique (John Wiley and Sons, Inc., New York, 2d edition, 1962), Chap. 5.
3. J. H. Singleton, J. Chem. Phys. 45, 2819 (1966).

4. J. H. Singleton, Private communication, 1971.
5. J. C. Batty and R. E. Stickney, J. Chem. Phys. 51, 4475 (1969).
6. J. C. Batty and R. E. Stickney, "Oxidation of Metals" (in press).
7. S. Dushman and J. M. Lafferty, op. cit., see Eq. (1.45).
8. For a detailed derivation of Eq. 9, see J. C. Batty and R. E. Stickney, J. Chem. Phys., loc. cit.
9. JANAF Tables of Thermochemical Data, D. R. Stull (ed.) (Dow Chemical Company, Midland, Michigan, 1965, and Second Addendum, 1967).
10. See Sections 10.1 and 10.2 of S. Dushman and J. M. Lafferty, op. cit.
11. H. F. Winters, D. R. Denison, D. G. Bills, and E. E. Donaldson, J. Appl. Phys. 34, 1810 (1963).

B. SIMPLIFIED EXPERIMENTAL METHOD FOR DETERMINING THE THERMODYNAMIC PROPERTIES OF CERTAIN VOLATILE SPECIES: APPLICATION TO ReO_2 AND ReO_3

1. Introduction

The enthalpies and free energies of formation of volatile species (e.g., oxides, halides, sulfides, etc.) are frequently determined from mass spectrometric measurements of the chemical composition of gas effusing from a Knudsen cell.[1,2] This method is especially important in the case of multicomponent systems at high temperatures in which the gas phase may include more than a single species. Application of the Knudsen cell method is a difficult and time-consuming process, however, because of complications arising from unwanted reactions of the substance with the cell, deviations from chemical equilibrium within the cell, transport of material from the cell by surface migration, and nonideal flow from the cell.[3] The purpose of this report is to explore the attributes of a method that eliminates many of these complications at the price of introducing others.

The method is based upon the apparent success of the quasi-equilibrium model in describing the reaction of O_2 with W and Mo surfaces at high temperature and low pressure.[4,5] (Note: the authors do not assume that the reader is familiar with the quasi-equilibrium model.) The method will be described and then tested by determining the free energies of formation, ΔG_f^o, of gaseous WO_2, WO_3, MoO_2, and MoO_3 from existing mass spectrometric measurements of the rates of evaporation of volatile oxides from W and Mo surfaces exposed to low-pressure O_2. The results of this test show that the present method yields values that agree satisfactorily with those obtained by the Knudsen-cell method. We shall demonstrate the application of the method to a case in which data on ΔG_f^o have not yet been obtained by other methods. Specifically, we shall determine the free energy of formation of gaseous ReO_2 and ReO_3 from the mass-

spectrometric measurements of Weber, Fusy, and Cassuto[6,7] for the evaporation of oxides from an Re surface. The advantages, disadvantages, and limitations of the method will also be considered.

2. Method

The experimental apparatus shown in Fig. III-5 permits mass-spectrometric measurements of the rates of evaporation of species from the surface of a solid or liquid sample. The sample, collimating aperture, and ion source of the mass spectrometer are arranged to allow a fraction of the evaporated species to pass directly from the

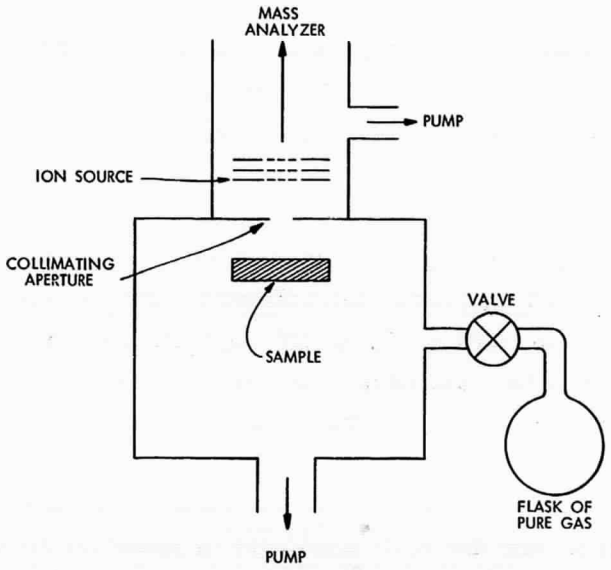

Fig. III-5. Typical apparatus for mass-spectrometric measurements of the evaporation rates of volatile species formed in the chemical reaction of a gas with a solid surface.

surface to the ion source. We shall assume that the pressure in the main chamber is sufficiently low (for example, $<1\times10^{-4}$ Torr) that collisions of the evaporated species with one another or with the background gas are negligible over the distance from the sample to the ion source. Various versions of this apparatus have been used in studies of the chemical composition of vapor emanating from the surface of single-component and multicomponent substances.[8] In such cases, the sample is commonly called a Langmuir source. Similar apparatus also have been employed in studies of chemical reactions of gases (or vapors) with solids or liquids.[8] The gas may be supplied either by molecular beam techniques or, as shown in Fig. III-5, by "leaking" gas into the chamber through a valve which may be adjusted to obtain the desired pressure.

For simplicity, we shall restrict our considerations to cases in which the sample is a single-component solid, M, and the gas contains only one reactive element, X. (Note: we should emphasize that these restrictions are simplifications rather than inherent limitations of the method; i.e., the method may be applied to multicomponent condensed and gaseous systems.) Hence, the volatile species formed in the reaction of the gas with the solid will be of the form $M_xX_y(g)$. Let us tentatively assume that the properties of the flux of reaction products emanating from the surface are identical to the corresponding properties of the flux of species from an ideal Knudsen cell at the temperature of the sample. (The underlying details of this assumption will be examined.) A consequence of this assumption is that the rate of evaporation of a particular species M_xX_y will be equal to the rate of effusion of the same species from a hypothetical Knudsen cell at the temperature of the sample. For an ideal Knudsen cell, the effusion rate of species i may be expressed[9] as

$$Z_i = p_i(2\pi m_i kT)^{-1/2}, \tag{1}$$

where p_i is the equilibrium partial pressure of species i within the cell, m_i is the molecular mass of i, k is Boltzmann's constant, and T is the cell temperature. The partial pressures of the various species in the cell are related through the equilibrium constants, K_p. For example, if the stoichiometric equations are expressed by the general form

$$xM(c) + yX(g) \rightleftharpoons M_xX_y(g), \tag{2}$$

then the corresponding equilibrium constants may be written[10] as

$$K_p = \exp\left(-\Delta G^o_{M_xX_y}/RT\right) = p_{M_xX_y}/p_X^y, \tag{3}$$

where $G^o_{M_xX_y}$ is the free energy of formation of $M_xX_y(g)$ from M(c) and X(g) at temperature T and unit pressure. With the aid of Eq. 1, this may be rewritten as

$$K_p = \exp\left(-\Delta G^o_{M_xX_y}/RT\right) = (2\pi kT)^{(1-y)/2}\left[\frac{m_{M_xX_y}}{m_X^y}\right]^{1/2}\frac{Z_{M_xX_y}}{Z_X^y}. \tag{4}$$

Since the evaporation rates are assumed to be equal to the corresponding values of the effusion rates, the right-hand side of Eq. 4 may be evaluated if T is measured and if the evaporation rates are determined by mass-spectrometric measurements. The procedures for converting mass spectrometer ion currents to evaporation or effusion rates have been described by other investigators.[1, 2]

We should point out that the free energy appearing in Eqs. 3 and 4 does not correspond directly to the conventional free energy of formation, $\left(\Delta G^{o}_{M_xX_y}\right)_f$, if the accepted reference state of the gas is $X_2(g)$, rather than X(g). In such cases, the relation between $\Delta G^{o}_{M_xX_y}$ for the reaction described by Eq. 2 and $\left(\Delta G^{o}_{M_xX_y}\right)_f$ for the conventional formation reaction,

$$xM(c) + y/2\ X_2(g) \rightleftharpoons M_xX_y(g), \tag{5}$$

is simply,

$$\Delta G^{o}_{M_xX_y} = \left(\Delta G^{o}_{M_xX_y}\right)_f - y\left(\Delta G^{o}_{X}\right)_f, \tag{6}$$

where $\left(\Delta G^{o}_{X}\right)_f$ is the free energy of formation of X(g) from $X_2(g)$ at temperature T and unit pressure. By substituting Eq. 6 in Eq. 4 and solving for $\left(\Delta G^{o}_{M_xX_y}\right)_f$, we obtain

$$\left(\Delta G^{o}_{M_xX_y}\right)_f = y\left(\Delta G^{o}_{X}\right)_f - RT \ln \left\{(2\pi kT)^{(1-y)/2} \left[\frac{m_{M_xX_y}}{m_X^y}\right]^{1/2} \frac{Z_{M_xX_y}}{Z_X^y}\right\}, \tag{7}$$

where it is assumed that $\left(\Delta G^{o}_{X}\right)_f$ may be found in existing thermochemical tables, such as the JANAF Tables.[11]

3. Test Cases: WO_2, WO_3, MoO_2, and MoO_3

As a test of the validity of the present method, we shall consider two systems (tungsten-oxygen and molybdenum-oxygen for which experimental data have been obtained both with apparatus similar to that shown in Fig. III-5 and with more conventional apparatus (e.g., Knudsen cells).

Schissel and Trulson[12] used apparatus like that shown in Fig. III-5 to measure the rates of evaporation of volatile oxides from a tungsten surface exposed to gaseous O_2 at $\sim 2 \times 10^{-4}$ Torr. By substituting their data on the evaporation rates of O and WO_2 in Eq. 7, we obtain the values of $\left(\Delta G^{o}_{WO_2}\right)_f$ listed in Table III-1. The temperature range is limited by the fact that only for $2000°K \leq T \leq 2900°K$ were Schissel and Trulson able to measure both Z_{WO_2} and Z_O. The values for $\left(\Delta G^{o}_{WO_3}\right)_f$ listed in Table III-1 were obtained in a similar manner, but in this case the temperature range is limited to $2000°K \leq T \leq 2300°K$.

The same procedure was applied to Steele's measurements[13] of the evaporation rates of volatile oxides from a molybdenum surface exposed to O_2 at $\sim 5 \times 10^{-5}$ Torr. The

Table III-1. Comparison of the results for ΔG_f^o obtained by the present method with the corresponding values listed in the JANAF Tables.

ΔG_f^o (kcal/mole)												
T (°K)	$WO_2(g)$			$WO_3(g)$			$MoO_2(g)$			$MoO_3(g)$		
	This report	JANAF	Diff.	This report	JANAF	Diff.	This report	JANAF	Diff.	This report	JANAF	Diff.
1900	—	—	—	—	—	—	-17.31	-19.61	2.30	-57.69	-59.48	1.79
2000	-5.52	-0.89	-4.63	-42.61	-43.37	0.76	-17.99	-20.29	2.30	-56.72	-58.00	1.28
2100	-7.23	-1.67	-5.56	-43.31	-41.99	-1.32	-18.98	-20.94	1.96	-55.99	-56.51	0.52
2200	-7.31	-2.44	-4.87	-41.81	-40.60	-1.21	-18.87	-21.58	2.51	-53.50	-55.01	1.51
2300	-6.46	-3.19	-3.27	-39.44	-39.20	-0.24	-19.62	-22.19	2.57	—	—	—
2400	-5.25	-3.93	-1.32	—	—	—	-20.52	-22.78	2.26	—	—	—
2500	-4.92	-4.66	-0.26	—	—	—	-21.44	-23.36	1.92	—	—	—
2600	-5.24	-5.36	0.12	—	—	—	—	—	—	—	—	—
2700	-6.37	-6.05	-0.32	—	—	—	—	—	—	—	—	—
2800	-6.98	-6.73	-0.25	—	—	—	—	—	—	—	—	—
2900	-9.43	-7.39	-2.04	—	—	—	—	—	—	—	—	—
Average Difference			-2.24			-0.50			2.26			1.27
JANAF Uncertainty			±7			±7			±5			±5

results for $\left(\Delta G^{o}_{MoO_2}\right)_f$ and $\left(\Delta G^{o}_{MoO_3}\right)_f$ are listed in Table III-1.

For comparison, we have included in Table III-1 the corresponding free energies of formation listed in the JANAF Tables as being the most reliable values on the basis of existing experimental data. Notice that the average differences between the values determined by the present method and the accepted JANAF values are well within the uncertainties estimated by the editors of the JANAF Tables. These results indicate that the present method is valid for the W-O and Mo-O systems.

4. Results for ReO_2 and ReO_3

Although the thermochemical properties of Re(g) and ReO(g) have been tabulated,[14] we are not aware of tabulations for ReO_2(g) and ReO_3(g). It appears that the existing experimental data on ReO_2 and ReO_3 are not sufficient for formulating tables on the basis of conventional methods.[6,7,15-18] Therefore, it seems worthwhile to demonstrate that an appropriate tabulation can be derived by applying the present method to the mass-spectrometric data of Weber, Fusy, and Cassuto[6,7] on the evaporation rates of oxides from a rhenium surface exposed to O_2 at pressures in the range 5×10^{-5}-3×10^{-4} Torr.

Pertinent experimental data of Weber et al.[6,7] are given in Table III-2, where p'_{O_2} is the partial pressure of O_2 in the test chamber, Z_i is the measured evaporation rate of species i, and ΔG^{o}_{f} is the result obtained by substituting these values of Z_i in Eq. 7. The conventional second-law and third-law methods[1,2,19,20] may be applied to these results to obtain estimates of the enthalpies and free energies of formation of ReO_2(g) and ReO_3(g) at standard conditions (that is, 298.15°K and 1 atm). The results of the second-law analysis proved to be unreliable, because of the limited temperature range of the experimental data and other inherent difficulties of the method.[19] The third-law analysis was based on rigid-rotator, harmonic-oscillator models[21] of ReO_2 and ReO_3, with the molecular constants as specified in Table III-3. The resulting computed values for the free-energy functions are given in Table III-4, and enthalpies of formation at standard conditions are listed in Table III-5. Using the values given in Tables III-4 and III-5, we have constructed Tables III-6 and III-7 which express the properties of ReO_2(g) and ReO_3(g) in the format of the JANAF Tables.[11]

5. Discussion

Since the present method yields satisfactory results for the dioxides and trioxides of W and Mo, it seems reasonable to expect that it also provides reliable results for ReO_2(g) and ReO_3(g). The uncertainties associated with the resulting thermochemical property values are greater, however, in the case of the rhenium oxides, because of the absence of experimental data on their molecular structure. Particularly crucial

Table III-2. Summary of experimental data of Weber, Fusy, and Cassuto and the resulting estimates of ΔG_f^o based on the present method (Eq. 7).

T (°K)	p'_{O_2} (Torr)	O(g)	ReO_2(g)		ReO_3(g)	
		(a) Z_O (atoms/cm^{2}s)	(c) Z_{ReO_2} (molec./cm^{2}s)	$\left(\Delta G^o_{ReO_2}\right)_f$ (kcal/mole)	(b) Z_{ReO_3} (molec./cm^{2}s)	$\left(\Delta G^o_{ReO_3}\right)_f$ (kcal/mole)
2050	3×10^{-4}	4.8×10^{15}	6.1×10^{13}	-1.14	4.5×10^{14}	-51.27
	2×10^{-4}	4.0×10^{15}			1.90×10^{14}	-49.99
	1×10^{-4}	2.85×10^{15}			4.5×10^{13}	-48.26
	5×10^{-5}	1.90×10^{15}			1.05×10^{13}	-47.29
2195	3×10^{-4}	1.18×10^{10}	5.5×10^{13}	-1.44	1.35×10^{14}	-50.63
	2×10^{-4}	9.4×10^{15}			5.7×10^{13}	-49.84
	1×10^{-4}	6.0×10^{15}			1.16×10^{13}	-48.77
	5×10^{-5}	3.8×10^{15}			2.40×10^{12}	-47.88
2330	3×10^{-4}	2.15×10^{16}	2.5×10^{13}	0.27	3.3×10^{13}	-49.87
	2×10^{-4}	1.62×10^{16}			1.45×10^{13}	-49.99
	1×10^{-4}	1.00×10^{16}			3.5×10^{12}	-50.11

(a) Data reported by Weber and Cassuto.[7]

(b) Revised data of Weber, Fusy, and Cassuto[6] obtained through private communication with the authors. These data differ slightly from the data reported in ref. 6 because they are based on a more reliable evaluation (i.e., weight-loss measurements) of the calibration factor used to compute the evaporation rate, Z_{ReO_3}, from the mass spectrometer ion current, $I_{ReO_3^+}$.

(c) Revised data of Weber, Fusy, and Cassuto.[6] In this case, the callibration factor for computing Z_{ReO_2} from $I_{ReO_2^+}$ has been estimated by multiplying the ReO_3 calibration factor [footnote (b)] by the ratio of the ReO_2 and ReO_3 ionization cross sections, with this ratio being estimated on the basis of the Otvos-Stevenson approximation [J. Am. Chem. Soc. 78, 546 (1956)].

Table III-3. Assumed values for the molecular properties of $ReO_2(g)$ and $ReO_3(g)$.

Property	Symbol	Units	ReO_2	ReO_3	Reference
Molecular Weight	M	–	218.2	234.2	a
Configuration	–	–	Bent	Pyramidal	b
Point Group	–	–	C_{2v}	C_{3v}	c
Symmetry Number	σ	–	2	3	c
Bond Distance Re-O	r_e	A	1.77	1.77	d
Bond Angle O-Re-O	2α	deg	105	105	b
Bond Stiffness of Monoxide	k_e	dyn $cm^{-1} \times 10^5$	7.00	7.00	e
Principal Moments of Inertia	I_A	$gcm^2 \times 10^{-38}$	0.53	1.37	c
	I_B	$gcm^2 \times 10^{-38}$	1.05	1.37	c
	I_C	$gcm^2 \times 10^{-38}$	1.58	2.08	c
Vibrational Levels and Multiplicities	ω_1	cm^{-1}	891(1)	881(1)	f
	ω_2	cm^{-1}	394(1)	332(1)	f
	ω_3	cm^{-1}	907(1)	910(2)	f
	ω_4	cm^{-1}	–	419(2)	f
Ground-State Quantum Weight	g_o	–	2	2	g

a. NBS Technical Note No. 270-4.

b. Based on Hayes' extension of Walsh's criteria [J. Phys. Chem. 70, 3740 (1966)]; see also Charkin [Zh. Strukt. Khim. 10, No. 4, 754 (1969)] and Nagarajan [Bull. Soc. Chim. Belg. 73, 655 (1964)].

c. See Herzberg (ref. 21, pages 1-14 and 508).

d. Mean of 6 values quoted by Sutton (Tables of Interatomic Distances and Configuration in Molecules and Ions (and Supplement), Chem. Soc. Lond. Spec. Pub. No. 18, 1965).

e. Estimated using Badger's rule [J. Chem. Phys. 2, 128 (1934)].

f. Calculated assuming valence forces, see Herzberg (ref. 21, pages 168-177) and Schick (ref. 14, Vol. 1).

g. Ground state assumed to be doublet; see G. Herzberg, Molecular Spectra and Molecular Structure III, Electronic Spectra and Electronic Structure of Polyatomic Molecules (D. Van Nostrand Company, New York, 1945, page 340).

Table III-4. Thermodynamic functions for $ReO_2(g)$ and $ReO_3(g)$ based on the assumed molecular properties listed in Table III-2. (Calculated from Stull and Prophet (ref. 19, pp. 388-389).)

T (°K)	$ReO_2(g)$		$ReO_3(g)$	
	$-(G^o-H^o_o)/T$ (cal/mole°K)	$(H^o-H^o_o)/T$ (cal/mole°K)	$-(G^o-H^o_o)/T$ (cal/mole°K)	$(H^o-H^o_o)/T$ (cal/mole°K)
298.15	58.145	8.840	59.747	10.319
500	62.963	9.854	65.612	12.436
1000	70.330	11.369	75.258	15.306
1500	75.091	12.088	81.741	16.618
2000	78.629	12.494	86.631	17.351
2500	81.446	12.753	90.557	17.816
3000	83.788	12.933	93.835	18.137
3500	85.792	13.064	96.649	18.371
4000	87.544	13.164	99.115	18.550
4500	89.099	13.243	101.308	18.691
5000	90.498	13.307	103.283	18.804
5500	91.769	13.360	105.080	18.898
6000	92.933	13.404	106.728	18.977

Table III-5. Determination of the standard enthalpies of formation of $ReO_2(g)$ and $ReO_3(g)$ by the third law method.

T (°K)	$ReO_2(g)$			$ReO_3(g)$		
	(a) $\Delta\left(\frac{G^o - H^o_{298}}{T}\right)$ (cal/mole°K)	(b) log K_p	(c) $\Delta H^o_{f_{298}}$ (kcal/mole)	(a) $\Delta\left(\frac{G^o - H^o_{298}}{T}\right)$ (cal/mole°K)	(b) log K_p (av)	(c) $\Delta H^o_{f_{298}}$ (kcal/mole)
2050	-6.942	0.121	13.10	13.374	5.248	-76.6
2195	-6.796	0.143	13.48	13.445	4.909	-78.7
2330	-6.665	-0.024	15.80	13.508	4.691	-79.1
$\Delta H^o_{f_{298}}$		Average	14.13		Average	-78.13

(a) Values of free-energy function for Re(c) from Schick (ref. 14, Table 223), for $O_2(g)$ from JANAF Tables,[11] and for $ReO_2(g)$ and $ReO_3(g)$ from Table III-4.

(b) From use of Eq. 7 and data of Weber, Fusy, and Cassuto[6, 7] (see Table III-2).

(c) From the relationship $\frac{\Delta H^o_{f_{298}}}{T} = -R \ln K_p - \Delta\left(\frac{G^o - H^o_{298}}{T}\right)$ (ref. 20).

Table III-6. Thermodynamic properties of ReO_2(g).

	gibbs/mol			kcal/mol			
T, °K	C_p°	S°	$-(G^\circ-H^\circ_{298})/T$	$H^\circ-H^\circ_{298}$	ΔHf°	ΔGf°	Log K_p
0.00	0.000	0.000	INFINITE	-2.639	14.876	14.876	INFINITE
298.15	10.434	66.986	66.986	0.000	14.130	11.418	-8.369
300.00	10.455	67.050	66.986	0.019	14.125	11.401	-8.309
400.00	11.409	70.196	67.408	1.119	13.868	10.530	-5.753
500.00	12.076	72.818	68.235	2.291	13.702	9.713	-4.245
600.00	12.530	75.063	69.191	3.523	13.537	8.930	-3.253
700.00	12.844	77.019	70.172	4.793	13.377	8.176	-2.552
800.00	13.065	78.790	71.138	6.089	13.211	7.444	-2.033
900.00	13.227	80.298	72.072	7.404	13.036	6.733	-1.635
1000.00	13.347	81.699	72.965	8.733	12.851	6.044	-1.320
1100.00	13.438	82.975	73.818	10.072	12.651	5.373	-1.067
1200.00	13.510	84.148	74.631	11.420	12.438	4.720	-0.859
1300.00	13.566	85.231	75.403	12.774	12.210	4.085	-0.686
1400.00	13.612	86.238	76.143	14.133	11.966	3.470	-0.541
1500.00	13.649	87.179	76.848	15.496	11.705	2.871	-0.418
1600.00	13.680	88.061	77.521	16.862	11.428	2.293	-0.313
1700.00	13.705	88.891	78.166	18.232	11.135	1.730	-0.222
1800.00	13.727	89.675	78.784	19.603	10.821	1.185	-0.143
1900.00	13.745	90.418	79.377	20.977	10.489	0.662	-0.076
2000.00	13.761	91.123	79.947	22.352	10.138	0.151	-0.016
2100.00	13.774	91.795	80.495	23.729	9.767	-0.337	0.035
2200.00	13.786	92.436	81.023	25.107	9.375	-0.809	0.080
2300.00	13.797	93.049	81.533	26.487	8.964	-1.264	0.120
2400.00	13.806	93.636	82.025	27.867	8.530	-1.699	0.154
2500.00	13.814	94.200	82.501	29.248	8.074	-2.115	0.184
2600.00	13.821	94.742	82.961	30.630	7.597	-2.514	0.211
2700.00	13.827	95.264	83.407	32.012	7.096	-2.892	0.234
2800.00	13.833	95.767	83.840	33.395	6.573	-3.255	0.254
2900.00	13.838	96.252	84.259	34.779	6.027	-3.597	0.271
3000.00	13.843	96.722	84.667	36.163	5.458	-3.919	0.285
3100.00	13.847	97.176	85.063	37.547	4.864	-4.218	0.297
3200.00	13.851	97.615	85.449	38.932	4.247	-4.504	0.307
3300.00	13.854	98.042	85.824	40.318	3.608	-4.766	0.315
3400.00	13.858	98.455	86.189	41.703	2.941	-5.011	0.322
3500.00	13.861	98.857	86.546	43.089	-3.686	-5.127	0.320
3600.00	13.863	99.247	86.893	44.476	-4.377	-5.102	0.309
3700.00	13.866	99.627	87.232	45.862	-7.073	-5.056	0.298
3800.00	13.868	99.997	87.563	47.249	-7.771	-4.989	0.286
3900.00	13.870	100.357	87.887	48.636	-8.472	-4.909	0.275
4000.00	13.872	100.709	88.203	50.023	-9.177	-4.810	0.262
4100.00	13.874	101.051	88.512	51.410	-9.885	-4.690	0.250
4200.00	13.876	101.385	88.814	52.798	-10.594	-4.555	0.237
4300.00	13.877	101.712	89.111	54.185	-11.307	-4.403	0.223
4400.00	13.879	102.031	89.401	55.573	-12.022	-4.236	0.210
4500.00	13.880	102.343	89.685	56.961	-12.739	-4.051	0.196
4600.00	13.881	102.648	89.963	58.349	-13.458	-3.850	0.182
4700.00	13.882	102.947	90.236	59.738	-14.179	-3.630	0.168
4800.00	13.884	103.239	90.504	61.126	-14.902	-3.403	0.154
4900.00	13.885	103.525	90.767	62.514	-15.627	-3.150	0.140
5000.00	13.886	103.806	91.025	63.903	-16.353	-2.892	0.126
5100.00	13.887	104.081	91.278	65.292	-17.081	-2.612	0.111
5200.00	13.887	104.350	91.527	66.680	-17.811	-2.325	0.097
5300.00	13.888	104 615	91.772	68.069	-18.541	-2.019	0.083
5400.00	13.889	104.875	92.012	69.458	-19.273	-1.704	0.068
5500.00	13.890	105.129	92.248	70.847	-20.005	-1.371	0.054
5600.00	13.890	105.380	92.480	72.236	-20.740	-1.022	0.039
5700.00	13.891	105.626	92.709	73.625	-21.475	-0.668	0.025
5800.00	13.892	105.867	92.934	75.014	-22.211	-0.294	0.011
5900.00	13.892	106.105	93.155	76.404	-22.947	0.092	-0.005
6000.00	13.893	106.338	93.373	77.793	-192.089	1.407	-0.058

Table III-7. Thermodynamic properties of $ReO_3(g)$.

T, °K	gibbs/mol C_p°	S°	$-(G^\circ-H^\circ_{298})/T$	kcal/mol $H^\circ-H^\circ_{298}$	ΔHf°	ΔGf°	log K_p
0.00	0.000	0.000	INFINITE	-3.076	-78.787	-78.787	INFINITE
298.15	13.917	70.067	70.067	0.000	-78.130	-74.455	54.577
300.00	13.955	70.153	70.067	0.025	-78.134	-74.432	54.224
400.00	15.673	74.419	70.637	1.512	-78.336	-73.164	39.975
500.00	16.823	78.048	71.765	3.141	-78.435	-71.858	31.409
600.00	17.590	81.188	73.080	4.864	-78.486	-70.538	25.693
700.00	18.114	83.941	74.439	6.651	-78.518	-69.210	21.608
800.00	18.482	86.385	75.782	8.482	-78.548	-67.879	18.543
900.00	18.749	88.579	77.084	10.344	-78.583	-66.543	16.159
1000.00	18.948	90.565	78.335	12.230	-78.625	-65.202	14.250
1100.00	19.099	92.378	79.530	14.132	-78.681	-63.857	12.687
1200.00	19.216	94.045	80.671	16.048	-78.750	-62.507	11.384
1300.00	19.309	95.587	81.760	17.975	-78.834	-61.151	10.280
1400.00	19.384	97.021	82.799	19.910	-78.934	-59.786	9.333
1500.00	19.444	98.360	83.793	21.851	-79.052	-58.416	8.511
1600.00	19.495	99.617	84.743	23.798	-79.186	-57.034	7.790
1700.00	19.537	100.800	85.653	25.750	-79.339	-55.645	7.153
1800.00	19.572	101.918	86.526	27.705	-79.513	-54.248	6.586
1900.00	19.602	102.977	87.364	29.664	-79.707	-52.835	6.077
2000.00	19.628	103.983	88.170	31.626	-79.922	-51.418	5.618
2100.00	19.650	104.941	88.946	33.590	-80.158	-49.987	5.202
2200.00	19.670	105.856	89.694	35.556	-80.418	-48.543	4.822
2300.00	19.686	106.731	90.416	37.524	-80.699	-47.090	4.474
2400.00	19.701	107.569	91.113	39.493	-81.005	-45.621	4.154
2500.00	19.715	108.373	91.787	41.464	-81.335	-44.139	3.858
2600.00	19.726	109.147	92.440	43.436	-81.688	-42.645	3.584
2700.00	19.737	109.891	93.073	45.409	-82.067	-41.135	3.329
2800.00	19.746	110.609	93.686	47.384	-82.470	-39.615	3.092
2900.00	19.754	111.302	94.282	49.359	-82.899	-38.078	2.869
3000.00	19.762	111.972	94.861	51.335	-83.352	-36.524	2.660
3100.00	19.769	112.620	95.423	53.311	-83.832	-34.950	2.463
3200.00	19.775	113.248	95.970	55.288	-84.338	-33.369	2.279
3300.00	19.781	113.857	96.503	57.266	-84.868	-31.766	2.103
3400.00	19.786	114.447	97.022	59.245	-85.427	-30.149	1.938
3500.00	19.791	115.021	97.528	61.224	-93.949	-28.406	1.773
3600.00	19.795	115.578	98.022	63.203	-94.537	-26.527	1.610
3700.00	19.799	116.121	98.504	65.183	-95.130	-24.629	1.454
3800.00	19.803	116.649	98.974	67.163	-95.728	-22.712	1.306
3900.00	19.806	117.163	99.434	69.143	-96.329	-20.785	1.134
4000.00	19.810	117.665	99.884	71.124	-96.936	-18.842	1.029
4100.00	19.813	118.154	100.323	73.105	-97.548	-16.879	0.899
4200.00	19.815	118.632	100.754	75.087	-98.162	-14.905	0.775
4300.00	19.818	119.098	101.175	77.069	-98.780	-12.915	0.656
4400.00	19.820	119.554	101.587	79.051	-99.402	-10.912	0.542
4500.00	19.823	119.999	101.992	81.033	-100.028	-8.895	0.432
4600.00	19.825	120.435	102.388	83.015	-100.656	-6.863	0.326
4700.00	19.827	120.861	102.776	84.998	-101.288	-4.813	0.223
4800.00	19.828	121.279	103.157	86.981	-101.922	-2.760	0.125
4900.00	19.830	121.687	103.531	88.964	-102.558	-0.680	0.030
5000.00	19.832	122.088	103.899	90.947	-103.198	1.399	-0.061
5100.00	19.833	122.481	104.259	92.930	-103.840	3.502	-0.150
5200.00	19.835	122.866	104.613	94.913	-104.484	5.607	-0.235
5300.00	19.836	123.244	104.961	96.897	-105.128	7.734	-0.318
5400.00	19.837	123.615	105.303	98.881	-105.776	9.864	-0.399
5500.00	19.839	123.979	105.639	100.865	-106.424	12.012	-0.477
5600.00	19.840	124.336	105.970	102.849	-107.076	14.177	-0.553
5700.00	19.841	124.687	106.295	104.833	-107.728	16.342	-0.626
5800.00	19.842	125.032	106.615	106.817	-108.381	18.527	-0.698
5900.00	19.843	125.371	106.930	108.801	-109.036	20.724	-0.767
6000.00	19.844	125.705	107.241	110.786	-278.092	24.049	-0.875

is the shape of the $ReO_2(g)$ molecule, which is assumed here to be bent. If the $ReO_2(g)$ molecule is found to be linear, the free-energy function at 2000°K, for example, would be ~ -74.8 cal mole^{-1} °K^{-1} rather than the value -78.629 cal mole^{-1} °K^{-1} quoted in Table III-4. Aside from this possibility, we estimate uncertainties in the values of free-energy function arising from our assumptions of molecular configuration to be approximately ±1.5 cal mole^{-1} °K^{-1} for $ReO_2(g)$ and ±2.5 cal mole^{-1} °K^{-1} for $ReO_3(g)$. There are many other possible sources of error, and we shall assume that they may be represented approximately by assigning an uncertainty of ±300% to the experimentally determined evaporation rates, Z_i. Based on these estimates of the uncertainties, the present results for $\Delta H^o_{f_{298}}$ are 14 ± 8 kcal mole^{-1} for $ReO_2(g)$ and -78 ± 14 kcal mole^{-1} for $ReO_3(g)$.

Our confidence in the present values of $\Delta H^o_{f_{298}}$ is increased by the fact that the Re-O bond energies estimated[22] from these values agree well with earlier estimates by Brewer and Rosenblatt[23] and by Semenov and Ovchinnikov.[18] Specifically, values for the Re-O bond energy calculated from the present values of $\Delta H^o_{f_{298}}$ for $ReO_2(g)$ and $ReO_3(g)$ are 145 ± 4 and 147 ± 5 kcal mole^{-1}, whereas previous estimates[23, 18, 16] are 140 ± 7.5 kcal mole^{-1}, 148 ± 2.5 kcal mole^{-1} and 144 kcal mole^{-1}.

We believe that there are many gas-solid systems for which the present method would prove to be far easier to employ than the conventional Knudsen-cell method. The principal advantages of the present method are: (i) the construction of a Langmuir source is extremely simple in comparison with that of a Knudsen cell; (ii) many of the problems encountered with Knudsen cells[3] are eliminated. There are several disadvantages which should be discussed. First, the present method is limited to those chemical species that can be formed as volatile products in the reaction of a gas with a solid (or liquid). Furthermore, the rates of formation of the given species and a reference species (i.e., a species for which thermochemical data exist such as O(g)) must be sufficiently large to be detectable over a range of temperature and pressure throughout which the following conditions are satisfied: (i) the coverage (i.e., concentration) of adsorbed species on the surface must be sufficiently low that the thermodynamics of the reaction depends primarily on the properties of the pure solid rather than on the properties of a poorly defined surface layer, such as a thin, amorphous, oxide layer;[4, 5] (ii) the density of impinging gas molecules plus the density of the evaporated species must be so low that gas-phase collisions are negligible over the distance from the surface to the mass spectrometer; (iii) the evaporation coefficients of the given species and the reference species must be either unity or uniquely related.[24] Specifically, the quasi-equilibrium model is not valid in cases where the reaction involves either the Rideal-Eley mechanism[25] or a "slow" step resulting from localized adsorption sites (as may exist on nonmetallic surfaces, such as Si, Ge, and C) or from

localized reaction sites (e.g., surface defects or steps, such as the edges of the lamellae of graphite).

Clearly, the present method is not as general or as fundamental as the Knudsen-cell method, and it can lead to erroneous results if applied under conditions that are outside the range defined by the above-mentioned limitations. On the other hand, the simplicity of the method makes it an extremely attractive choice for cases that are within its range of validity.

6. Summary

Our objective has been to evaluate a simplified experimental method for determining the enthalpies and free energies of formation of volatile species that can be formed by gas-solid chemical reactions at high temperature and low pressure. The principal feature of the method is the replacement of the conventional Knudsen cell by a solid surface (i.e., a "Langmuir source") which is exposed to a specified gaseous environment at sufficiently low pressure that molecular flow conditions are attained. The rates of evaporation of species from the surface are determined by mass-spectrometric measurements in the same manner as for determinations of the rates of effusion of species from a Knudsen cell. The present method is essentially an extension of the Langmuir method[3b, 3d] from studies of vaporization of condensed phases to studies of gas-solid reactions under conditions in which the products are highly volatile.

We have tested the method by applying it to two cases for which experimental data have been obtained both by the present method and by more conventional methods. The results of these tests are affirmative, since the free energies of formation obtained by the present method for the dioxides and trioxides of W and Mo fall within the range of the corresponding values listed in the JANAF Tables. As an illustrative application of the method to a case for which data have not yet been obtained by conventional methods, we consider recent mass-spectrometric measurements of the reaction of gaseous O_2 with solid Re.[6,7] The resulting values of the thermochemical properties of $ReO_2(g)$ are given in Tables III-4, III-5, and III-6. Specifically, the standard enthalpy of formation, $\Delta H^o_{f_{298}}$, is computed to be 14 ± 8 kcal mole^{-1} for $ReO_2(g)$ and -78 ± 14 kcal mole^{-1} for $ReO_3(g)$.

Since the present method is a generalization of the Langmuir method, it suffers from the well-documented limitations of Langmuir sources.[3b,3d] These limitations and others have been considered, and we emphasize that serious errors may result if the method is applied without proper consideration of its limitations. On the other hand, the Knudsen-cell method also has many limitations,[1, 3a-3c] and we suggest that the present method will prove to be a much easier approach in some high-temperature thermochemical studies of volatile species that can be formed by gas-solid reactions (e.g., refractory-metal oxides and halides).

J. E. Franklin, R. E. Stickney

References

1. M. G. Inghram and J. Drowart, in "Proceeding of an International Symposium on High Temperature Technology, Asilomar, California, October 1959" (McGraw-Hill Publishing Company, New York, 1960), pp. 219-240.
2. R. T. Grimley, in J. L. Margrave (Ed.), The Characterization of High Temperature Vapors (John Wiley and Sons, Inc., New York, 1967), pp. 195-243.
3. For a discussion of the complications associated with Knudsen cells and Langmuir sources, see M. G. Inghram and J. Drowart, op. cit. and the following.
   (a) K. D. Carlson, in J. L. Margrave (Ed.), The Characterization of High Temperature Vapors (John Wiley and Sons, Inc., New York, 1967), pp. 115-129.
   (b) R. C. Paule and J. L. Margrave, ibid., pp. 130-151.
   (c) E. D. Cater, in R. A. Rapp (Ed.), Physico-chemical Measurements in Metal Research, Part 1, "Techniques of Metal Research" (Interscience Publishers, New York, 1970), Vol. 4, Part 1, pp. 21-94.
   (d) W. L. Winterbottom, ibid., pp. 95-129.
4. J. C. Batty and R. E. Stickney, J. Chem. Phys. 51, 4475 (1969).
5. J. C. Batty and R. E. Stickney, "Oxidation of Metals" (in press).
6. B. Weber, J. Fusy, and A. Cassuto, in K. Ogata and T. Hayakawa (Eds.), Recent Developments in Mass Spectroscopy (University Park Press, Baltimore, 1970), pp. 1319-1324.
7. B. Weber and A. Cassuto, J. Chimie Phys. (in press).
8. See references listed in Table 1 of ref. 1 and in Table 3-1 of R. F. Porter, in G. E. Campbell and E. M. Sherwood (Eds.), High Temperature Materials and Technology (John Wiley and Sons, Inc., New York, 1967), p. 63.
9. E. H. Kennard, Kinetic Theory of Gases (McGraw-Hill Publishing Company, New York, 1938).
10. K. Denbigh, in The Principles of Chemical Equilibrium (Cambridge University Press, London, 1955), pp. 138-141.
11. D. R. Strull (Ed.), JANAF Tables of Thermochemical Data, and Addenda 1966, 1967, and 1968 (Dow Chemical Co., Midland, Michigan, 1965.
12. P. O. Schissel and O. C. Trulson, J. Chem. Phys. 43, 737 (1965).
13. W. C. Steele, Technical Report AFML-TR-343, Part 3, April 1968.
14. H. L. Schick (Ed.), in Thermodynamics of Certain Refractory Compounds, Vols. 1 and 2 (Academic Press, Inc., New York, 1966).
15. M. H. Studier, J. Phys. Chem. 66, 189 (1962).
16. L. H. Rovner, A. Drowart, F. Degreve, and J. Drowart, Technical Report AFML-TR-68-200, July 1968.
17. Argonne National Laboratory, "Chemical Division Semi-Annual Report, January-June 1967," ANL-7375, pp. 95-134.
18. G. A. Semenov and K. V. Ovchinnikov, Zh. Obshch. Knim. 35, No. 9, 1517 (1965).
19. D. R. Stull and H. Prophet, in J. L. Margrave (Ed.), The Characterization of High Temperature Vapors (John Wiley and Sons, Inc., New York, 1967), pp. 359-424.
20. G. N. Lewis and M. Randall (revised by K. S. Pitzer and L. Brewer), Thermodynamics (McGraw-Hill Publishing Company, New York, 1961).
21. G. Herzberg, in Molecular Spectra and Molecular Structure II. Infrared and Raman Spectra of Polyatomic Molecules (D. Van Nostrand Company, Inc., New York, 1945).

22. The procedure for estimating bond energies from data on ΔH_f^o is described by G. Herzberg, in Molecular Spectra and Molecular Structure I. Spectra of Diatomic Molecules (D. Van Nostrand Company, Inc., New York, 1950), pp. 480-482.

23. L. Brewer and G. M. Rosenblatt, Chem. Rev. 61, 257 (1961).

24. The fundamental requirement is that the evaporation coefficients, ζ, satisfy the equation $\zeta_X^y / \zeta_{M_x X_y} = 1$. See ref. 4 and J. C. Batty and R. E. Stickney, Technical Report 473, Research Laboratory of Electronics, M.I.T., Cambridge, Mass., June 2, 1969.

25. For a discussion of the Rideal-Eley mechanism, see G. C. Bond, in Catalysis by Metals (Academic Press, Inc., New York, 1962), p. 128.